This article has been accepted for publication in a future issue of this journal, but has not been fully edited. Content may change prior to final publication. Citation information: DOI 10.1109/TII.2016.2516823, IEEE Transactions on Industrial Informatics

Adaptive Neuro Fuzzy Inference System Least Mean Square Based Control Algorithm for DSTATCOM

Manoj Badoni, Alka Singh, *Senior Member, IEEE* and Bhim Singh, *Fellow, IEEE*

***Abstract*—This paper proposes the real time implementation of a three phase distribution static compensator (DSTATCOM) using adaptive neuro fuzzy inference system least mean square (ANFIS-LMS) based control algorithm for compensation of current related power quality problems. This algorithm is verified for various functions of DSTATCOM such as harmonics compensation, unity power factor, load balancing and voltage regulation. The ANFIS-LMS based control algorithm is used for the extraction of fundamental active and reactive power components from non-sinusoidal load currents to estimate reference supply currents. Real time validation of the proposed control algorithm is performed on a developed laboratory prototype of a shunt compensator. The real time performance of shunt compensator with ANFIS-LMS based control algorithm is found satisfactory under steady state and dynamic load conditions. The performance of proposed control algorithm is also compared with fixed step LMS and variable step LMS (VSLMS) to demonstrate its improved performance.**

***Index Terms*—Adaptive filtering, adaptive neuro fuzzy inference system (ANFIS), harmonics compensation, power quality, unity power factor, voltage regulation.**

I. INTRODUCTION

THERE is an increased penetration of power electronics based loads in industries and domestic sector which inject harmonics in the distribution system. Additionally, poor power factor, load unbalancing and high neutral current are some of the power quality problems introduced by a variety of loads in the distribution system. Power quality problems such as waveform distortion are due to harmonics and load unbalancing, which cause undesirable burden on the distribution system. Many topologies have been developed for compensation of power quality problems which include the application of passive filters, active filters and hybrid filters. Active power filter devices are used for suppressing the effects of non-sinusoidal load current, regulating the distribution bus voltage, cancelling the effect of poor power factor and achieving balanced supply currents even under unbalanced load conditions. The active filters are also known as distribution static compensator (DSTATCOM). A DSTATCOM is normally a voltage source converter (VSC) based shunt compensator [1]-[3]. The implementation and control of DSTATCOM have become possible due to advancement in digital signal processors (DSPs) and self-commutating semiconductor devices [4]-[6]. An improvement in power quality is reported using several new control techniques.

An internal control of DSTATCOM is a prerequisite to achieve desired performance in steady state and dynamic conditions. Different techniques for extracting harmonics from distorted load current have been suggested by various authors. Instantaneous reactive power theory [7] is based on the calculation of active and reactive powers by converting three phase voltages and currents into two phases. This control technique does not work well under non-sinusoidal supply voltages [8]. Synchronous reference frame theory [9] is based on the conversion of three phase quantities into their dc counterparts and low-pass filters (LPFs) are realized for harmonic filtering [10]-[11]. It is difficult to estimate the optimum parameters of these LPFs with hysteresis current controller. Some other algorithms for extracting the reference currents have been developed and successfully implemented. These include instantaneous model reference adaptive control [12], single phase active-reactive power theory [13], software PLL based reference extraction [14], implicit closed-loop current control and resonant controller [15].Adaptive filtering [16]-[17] has also been recognized as powerful control technique for extracting reference sinusoidal current from distorted load current. The advantage of adaptive filtering control techniques is that they exhibit better response under transient conditions. A number of adaptive filtering algorithms are reported and have found application in control, communication and signal processing. Several authors have suggested algorithms based on least mean square (LMS)[18], variable least mean square (VLMS) adaptive filtering in control system and signal processing [19]-[20], fuzzy inference based VSLMS [21], block least mean square algorithm [22], artificial neural network (ANN) based adaptive control [23]-[24], and robust adaptive control strategy [25].

In this paper, an adaptive least mean square (LMS) algorithm is developed in which the step size parameters are updated using adaptive neuro fuzzy inference system

Manuscript received November 08, 2014; revised March 24, 2015, October 14, 2015, and December 01, 2015; accepted January 04, 2016.

M. Badoni and A. Singh are with the Department of Electrical Engineering, Delhi Technological University, Delhi, India (manojbadoni23@gmail.com, alkasingh.dr@gmail.com).

B. Singh is with the department of Electrical Engineering, Indian Institute of Technology, Delhi, India (bhimsingh7nc@gmail.com).

This article has been accepted for publication in a future issue of this journal, but has not been fully edited. Content may change prior to final publication. Citation information: DOI 10.1109/TII.2016.2516823, IEEE Transactions on Industrial Informatics

(ANFIS). An adaptive neuro fuzzy inference system least mean square (ANFIS-LMS) based control algorithm is developed using Matlab/Simulink and its effectiveness is verified experimentally. The extraction of sinusoidal reference current from distorted load current is achieved by controller action. The proposed algorithm is compared with fixed step LMS and variable step based VSLMS as suggested in [18], [19] and [20]. A major advantage of the proposed control algorithm is that it exhibits less static error and achieves fast convergence. The step size estimated using ANFIS learns faster and achieves less static error in fundamental weight estimation. The proposed control algorithm is used for the control of the shunt compensator and has the ability to improve various aspects of power quality such as harmonics compensation, voltage regulation, power factor correction and load balancing. An improved performance is achieved under steady state as well as dynamic load conditions with the ANFIS-LMS based adaptive technique.

II. System Configuration

Fig. 1 shows the schematic diagram of a three phase shunt compensator. A utility supply of 3-phase, 415V and 50 Hz feeds the load. Small line impedance (L_s-R_s) associated with utility acts as a feeder. The basic building block in the DSTATCOM is a voltage source converter (VSC), which is modeled using a universal bridge in Simulink library. The VSC consists of six insulated gate bipolar transistors (IGBTs) switches with anti-parallel diodes. The nonlinear load is modeled using uncontrolled rectifier with series R-L branch. The DSTATCOM is connected at PCC with the help of interfacing inductors (L_f), used to filter compensator currents. High switching frequency components generated by IGBTs are eliminated by resistive-capacitive (R_f-C_f) ripple filters. Simulation study of the proposed system is made using SPS (Sim Power System) tool-box in Matlab/Simulink and the real time validation of the ANFIS-LMS based control algorithm is carried out by developing a small scale prototype in the laboratory using DSP controller.

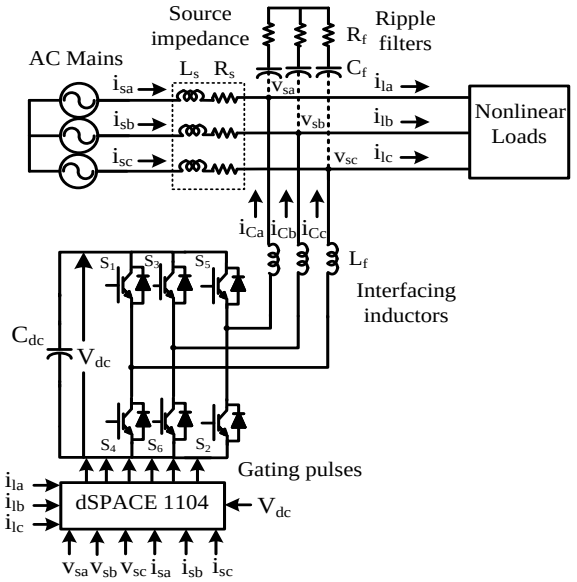

Fig. 1 System configuration of the shunt compensator

III. Control Algorithm

The detailed description of adaptive least mean square (LMS) technique is presented here, in which the step size parameter is updated using adaptive neuro fuzzy inference system (ANFIS). An adaptive neuro fuzzy inference system least mean square (ANFIS-LMS) based control algorithm is developed and its mathematical formulation is discussed. Both the LMS method and ANFIS structure are shown in Fig. 2 and Fig. 3 respectively. The complete block diagram of the control algorithm is shown in Fig. 4.

A. Estimation of Fundamental Active Power Components of Reference Supply Currents

An amplitude of PCC voltage (V_t) is calculated as,

$$V_t = \sqrt{2(v_{sa}^2 + v_{sb}^2 + v_{sc}^2)/3} \quad (1)$$

where v_{sa}, v_{sb} and v_{sc} are the sensed PCC phase voltages.

In-phase unit templates of PCC voltages u_{pa}, u_{pb} and u_{pc} are derived as,

$$u_{pa} = v_{sa}/V_t,\ u_{pb} = v_{sb}/V_t \text{ and } u_{pc} = v_{sc}/V_t \quad (2)$$

The difference (v_{de}) between the sensed (V_{dc}) and reference dc link voltage (V_{dc}^*) is calculated and passed through a PI (Proportional Integral) controller. The output of the PI controller is an active power component, which is used to maintain dc link voltage at reference value and meets VSC losses. At k^{th} sampling instant, the PI controller output is given as,

$$w_{ploss}(k) = w_{loss}(k-1) + k_{pd}\{v_{de}(k) - v_{de}(k-1)\} + k_{id}\big(v_{de}(k)\big) \quad (3)$$

where parameters w_{ploss}, k_{pd} and k_{id} are the PI controller output, proportional and integral gains respectively.

The non-sinusoidal load current is expressed at k^{th} sampling instant as,

$$i_l(k) = I_{lf}\sin\big(\omega k + \emptyset_f\big) + \sum_{h=5,7\ldots}^{\infty} I_{lh}\sin(h\omega k + \emptyset_h) = i_{lf}(k) + i_{lh}(k) \quad (4)$$

where I_{lf} and I_{lh} represent peak value corresponding to fundamental component and harmonic component of load current respectively. Angles $\emptyset_f$ and $\emptyset_h$ represent phase angles of fundamental and harmonic components of load current respectively.

The current corresponding to fundamental and harmonic components of load current can be further divided as,

$$i_{lf}(k) = I_{lf}\sin\omega k\cos\emptyset_f + I_{lf}\cos\omega k\sin\emptyset_f \quad (5)$$

$$i_{lh}(k) = I_{lh}\sin h\omega k\cos\emptyset_f + I_{lh}\cos h\omega k\sin\emptyset_f \quad (6)$$

Replacing $I_{lf}\cos\emptyset_f$, $I_{lf}\sin\emptyset_f$, $I_{lh}\cos\emptyset_f$ and $I_{lh}\sin\emptyset_f$ by weights w_{a1}, w_{b1}, w_{ah} and w_{bh} respectively, the new

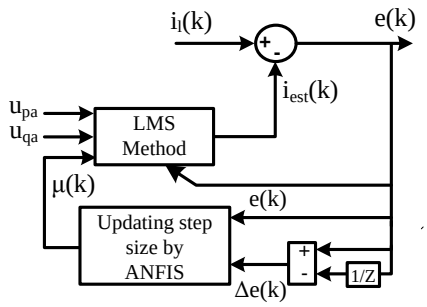

Fig. 2 Error minimization by ANFIS-LMS

This article has been accepted for publication in a future issue of this journal, but has not been fully edited. Content may change prior to final publication. Citation information: DOI 10.1109/TII.2016.2516823, IEEE Transactions on Industrial Informatics

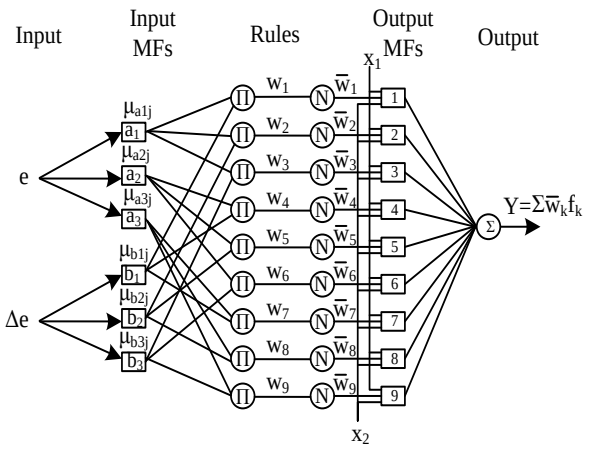

Fig. 3 Structure of nine rule ANFIS

equations are formed as,

$$i_{lf}(k) = w_{a1}\sin\omega k + w_{b1}\cos\omega k \quad (7)$$

$$i_{lh}(k) = w_{ah}\sin h\omega k + w_{bh}\cos h\omega k \quad (8)$$

where 'h' denotes the order of harmonics, $h = 5,7 \ldots . \infty$.

The estimated load current is computed from the optimum weights (w_{a1}, w_{b1}, w_{ah} and w_{bh}) expressed as,

$$i_{est}(k) = W^T X(k) \quad (9)$$

where the input vector $X(k)$ is given as,

$X(k) = [\sin\omega k \cos\omega k \ \sin 5\omega k \cos 5\omega k \ ...]^T$, which represents vector of unit in-phase and quadrature templates $[u_{pa}\ u_{qa}\ u_{5pa}\ u_{5qa}\ldots]^T$. The unit quadrature templates are calculated in next sub-section. The weight vector W^T is represented as, $W^T = [w_{a1}\, w_{b1} w_{a5}\, w_{b5} \ldots]$.

The error $e(k)$, between actual load current $i_l(k)$ and estimated load current $i_{est}(k)$ is given as,

$$e(k) = i_l(k) - W^T X(k) \quad (10)$$

The objective here is to minimize mean square error E[$e^2(k)$], which is achieved by finding the optimum weights. These weights are optimized by least mean square (LMS) method given as,

$$w(k+1) = w(k) + 2\mu e(k)X(k) \quad (11)$$

where 'μ' is the step size parameter. The convergence and stability of LMS method depend on the step size parameter. This method is used to find optimum weights so that the mean square error can be minimized. The step size parameter 'μ' can be kept fixed or variable. The disadvantage with fixed value of 'μ' is that the LMS algorithm is not able to achieve minimum static error with fast convergence rate. When 'μ' is high, the convergence is faster with increased static error. However, when 'μ' is small, convergence is slow with reduced static error.

To solve the contradiction between the convergence rate and steady state error, an ANFIS based variation of step size 'μ' is proposed in this paper. The structure of ANFIS is developed with two inputs, three membership functions (MFs) and nine rules as shown in Fig. 3. This represents both square and circular nodes, to identify different adaptive capabilities. The ANFIS structure uses first order Sugeno type fuzzy inference system [26]-[27]. The function of each layer of ANFIS structure is given as follows.

Layer 1: This is the fuzzification layer, having two inputs. One input of this layer is error (x_1=e(k)) between actual and estimated value of load current ($i_l(k) - W^T X(k)$) and other input is the change in error (x_2=Δe(k)). Each input function corresponds to three MFs and the shape of MFs is represented as square bracket. The internal structure of each square bracket represents trapezoidal and triangular MFs. Equations related to each MFs are given as,

$$\mu_{a1}(x_1) = \mu_{b1}(x_2) = \begin{cases} 0, & x > m_1 \\ \frac{m_1 - x}{m_1 - n_1}, & n_1 \le x \le m_1 \\ 1, & x < n_1 \end{cases} \quad (12)$$

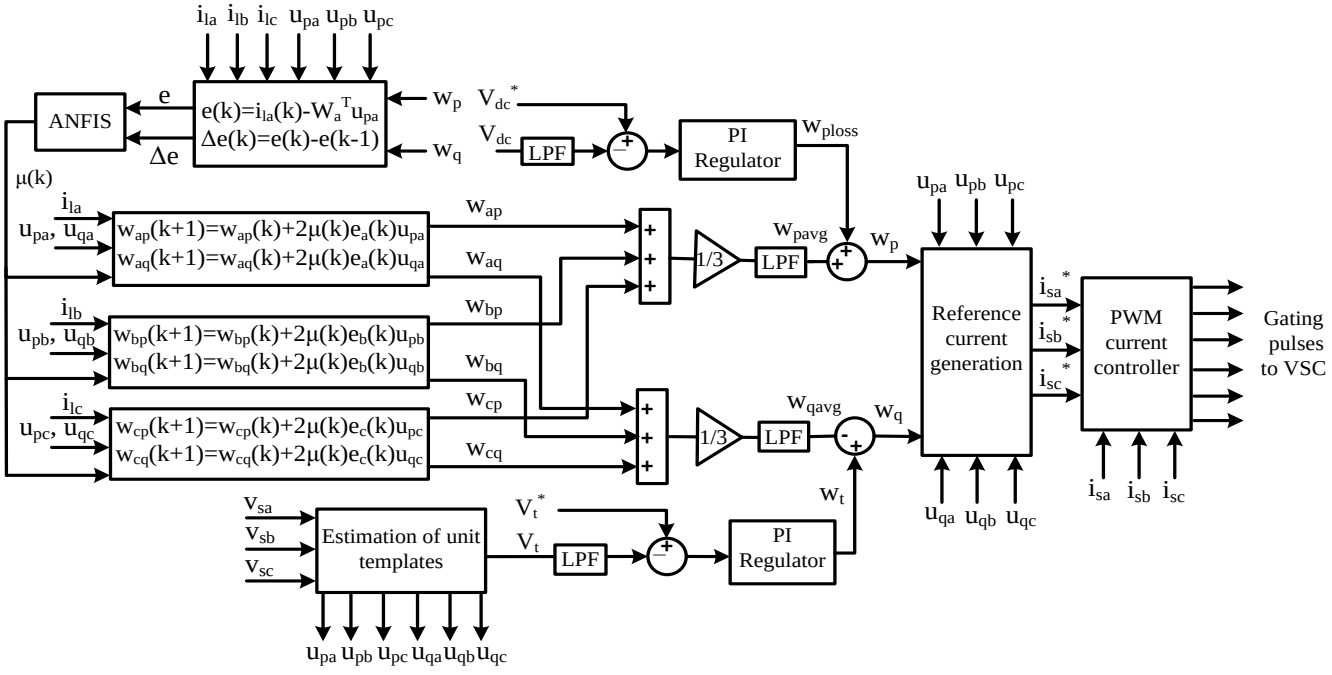

Fig. 4 Block diagram of ANFIS-LMS based control algorithm for DSTATCOM

This article has been accepted for publication in a future issue of this journal, but has not been fully edited. Content may change prior to final publication. Citation information: DOI 10.1109/TII.2016.2516823, IEEE Transactions on Industrial Informatics

$$\mu_{a2}(x_1) = \mu_{b2}(x_2) = \begin{cases} 0, & x \le m_1 \\ \frac{x-n_2}{p-n_2}, & n_2 < x \le p \\ \frac{m_2-x}{m_2-p}, & p < x < m_2 \\ 0, & x \ge m_2 \end{cases} \quad (13)$$

$$\mu_{a3}(x_1) = \mu_{b3}(x_2) = \begin{cases} 0, & x < m_1 \\ \frac{x-m_3}{n_3-m_3}, & m_3 \le x \le n_3 \\ 1, & x > n_3 \end{cases} \quad (14)$$

where $\{m_i, n_i\}$ are set of parameters, and value of i=1, 2, 3. The parameters $\{m_i, n_i\}$ change with the change in value of error and correspondingly generate the linguistic value of each MF. These parameters are known as *premise* parameters.

Layer 2: This layer is known as implication layer and each node in this layer is fixed node. This layer represented as Π and the output of each node of this layer is multiplication of its input signals,

$$w_k = \mu_{aij}(x_1)\,\mu_{bij}(x_2) \quad (15)$$

where k=1, 2,..9, i=1, 2, 3 and j=1, 2, 3. Each node in this layer represents firing strength of the rule.

Layer 3: Every node in this layer is also a fixed node and represented by N. This is also known as normalizing layer given as,

$$\bar{w}_k = w_k/(w_1 + w_2 + \cdots + w_9) \quad (16)$$

where k=1,2,….9 and output of each node in this layer is called the normalized firing strength.

Layer 4: This is known as defuzzifing layer and every node in this layer is adaptive. The nodes of this layer are represented by square shape and the node function is given as,

$$O_k = \bar{w}_k f_k = \bar{w}_k(p_k x_1 + q_k x_2 + r_k) \quad (17)$$

where p_k,q_k and r_k are the *consequence* parameters.

Layer 5: This is a single node layer represented by summation. The output of this layer represents the summation of all input signals. The node function for this layer is given as,

$$Y = \sum_{k=1}^{9} \bar{w}_k f_k \quad (18)$$

The ANFIS structure described above is used to compute the step size parameters μ(k), which is used to find optimum weight vector for LMS algorithm.

Learning of premise (m_i and n_i) and consequence parameters (p_k, q_k and r_k) in ANFIS structure is carried out with the hybrid learning algorithm [28]. This uses least square and gradient descent methods to find consequent and premise parameters respectively. The ANFIS structure proposed here, uses forward pass and backward pass learning algorithm. Suppose S, S_1 and S_2 represent total set of parameters, set of premise parameters and set of consequent parameters respectively, then in the forward pass S_1 is unchanged and S_2 is computed using least square error algorithm. The forward pass presents the input vector and node output to it. It can be calculated layer by layer till the corresponding data is obtained and process is repeated. Once all data have been obtained, the value of consequence parameter set S_2 can be obtained and it also computes error signal for each training pair.

In the backward pass, S_2 is unchanged and parameters of S_1 are computed using gradient descent algorithm such as back-propagation. The error signal computed above propagates from output towards input end. The gradient vector is found for each training data entry and updating of input parameters is performed with gradient descent algorithm.

The step size parameter μ(k) computed from ANFIS structure is used in LMS method given in (11). This method is used to extract fundamental active power weights (w_{ap}, w_{bp} and w_{cp}) corresponding to the load currents. The average weight (w_{pavg}) of active power weights is calculated as,

$$w_{pavg} = (w_{ap} + w_{bp} + w_{cp})/3 \quad (19)$$

This average weight (w_{pavg}) is added with the output of DC bus PI controller (w_{pdc}) and reference active power weight (w_p) is calculated as,

$$w_p = w_{pavg} + w_{pdc} \quad (20)$$

Active power components of reference supply currents (i_{pa}^*, i_{pb}^* and i_{pc}^*) are estimated from the reference active power weight (w_p) and unit inphase templates (u_{pa}, u_{pb} and u_{pc}) as,

$$i_{pa}^* = w_p u_{pa},\ i_{pb}^* = w_p u_{pb} \text{ and } i_{pc}^* = w_p u_{pc} \quad (21)$$

These active power components of reference supply currents are used to calculate total reference supply currents.

B. Estimation of Fundamental Reactive Power Component of Reference Supply Currents

Unit quadrature templates (u_{qa}, u_{qb} and u_{qc}) of PCC voltages are calculated from unit inphase templates (u_{pa}, u_{pb} and u_{pc}) as,

$$u_{qa} = -u_{pb}/\sqrt{3} + u_{pc}/\sqrt{3} \quad (22)$$

$$u_{qb} = \sqrt{3}\,u_{pa}/2 + (u_{pb} - u_{pc})/2\sqrt{3} \quad (23)$$

$$u_{qc} = -\sqrt{3}\,u_{pa}/2 + (u_{pb} - u_{pc})/2\sqrt{3} \quad (24)$$

Another PI controller in control algorithm is used to regulate voltage at PCC. The input for PI controller is error (v_{te}) between actual PCC voltage (V_t) and its reference value (V_t^*). The output for PI controller at k^{th} sampling instant is given as,

$$w_t(k) = w_t(k-1) + k_{pq}\{v_{te}(k) - v_{te}(k-1)\} + k_{iq}\big(v_{te}(k)\big) \quad (25)$$

where parameters w_t, k_{pq} and k_{iq} are the PI controller output, proportional and integral gains for voltage regulation respectively.

The weights (w_{aq}, w_{bq} and w_{cq}) corresponding to fundamental reactive power component of load current are extracted by ANFIS-LMS algorithm using (11) and average magnitude (w_{qavg}) is calculated as,

$$w_{qavg} = (w_{aq} + w_{bq} + w_{cq})/3 \quad (26)$$

The output of ac bus PI controller (w_t) is a leading quadrature power component, which is used to compensate voltage drop in supply side impedance and loading of the system. The reference reactive power weight (w_q) is calculated as,

$$w_q = w_t - w_{qavg} \quad (27)$$

The reference fundamental reactive power components of supply currents (i_{qa}^*, i_{qb}^* and i_{qc}^*) are estimated from the reference reactive power weight (w_q) and unit quadrature templates as,

$$i_{qa}^* = w_q u_{qa},\ i_{qb}^* = w_q u_{qb} \text{ and } i_{qc}^* = w_q u_{qc} \quad (28)$$

The estimated active and reactive power components are added to generate total reference supply currents.

C. Estimation of Reference Supply Currents and Generation of Switching Pulses

This article has been accepted for publication in a future issue of this journal, but has not been fully edited. Content may change prior to final publication. Citation information: DOI 10.1109/TII.2016.2516823, IEEE Transactions on Industrial Informatics

The summation of reference active and reactive power components of (21) and (28) are considered as reference currents (i_{sa}^*, i_{sb}^* and i_{sc}^*). These reference currents are compared with the sensed supply currents (i_{sa}, i_{sb} and i_{sc}) and current errors (i_{sae}, i_{sbe} and i_{sce}) are evaluated. These current errors are passed through pulse width modulation (PWM) current controller for the generation of switching pulses for three-phase VSC used as DSTATCOM.

IV. Simulation Results And Discussion

A simulation model of the system using proposed ANFIS-LMS based control algorithm, is developed in Matlab/Simulink environment using Sim Power System (SPS) tool-box. Performance of the control algorithm for a shunt compensator is verified for power factor correction (PFC) and voltage regulation modes under nonlinear load for varying load condition such as unbalancing and load change. The performance of DSTATCOM under various operating conditions are shown in the following section and the detailed simulation parameters are given in Appendix-A.

A. Performance of DSTATCOM in PFC Mode

Fig. 5 depicts the dynamic performance of the shunt compensator for power factor correction (PFC) mode under unbalanced load condition. In this, the waveforms of PCC voltages (v_s), supply currents (i_s), load currents (i_{la}, i_{lb} and i_{lc}), compensator currents (i_{Ca}, i_{Cb} and i_{Cc}) and dc link voltage (v_{dc}) are represented. An unbalancing is created in load current during t=0.74s to t=0.8s, when phase 'c' is disconnected. During load unbalancing it is observed that the supply currents are sinusoidal and balanced with reduced amplitude. The voltage at dc link is regulated and achieves reference value of 750V. After t=0.8s, phase 'c' of load is re-connected and it is observed that dc link voltage achieves its reference value within a cycle.

Fig. 6 represents harmonic spectra for phase 'a' of PCC voltage (v_{sa}), supply current (i_{sa}) and load current (i_{la}) along with their waveforms. Figs. 6(a)-(c) show 2.39%, 2.57 % and 26.66% THDs in phase 'a' of PCC voltage (v_{sa}), supply current (i_{sa}) and load current (i_{la}) respectively. The DSTATCOM with the help of proposed control is able to achieve 2.57% THD in supply current which lies within the limit specified by IEEE-519 standard, even when load current THD is around 26.66%. Fig. 5 and Fig. 6 depict satisfactory performance of DSTATCOM with ANFIS-LMS based control algorithm under varying load condition in PFC mode.

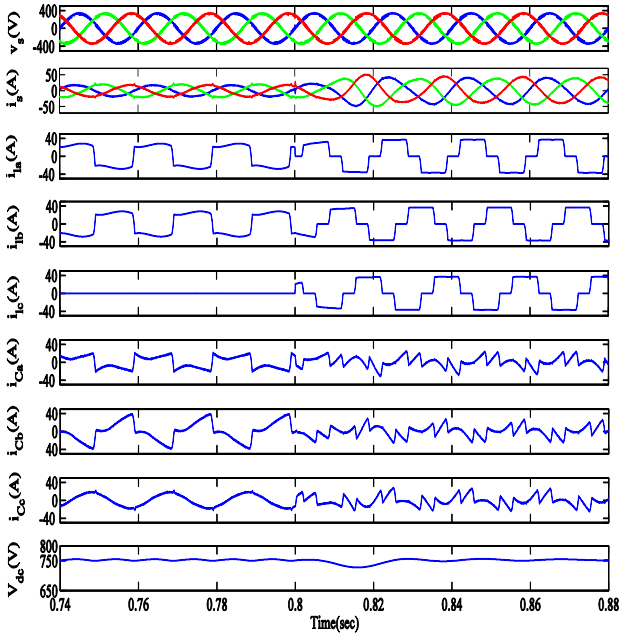

Fig. 5 Performance of compensator for PFC mode under varying non-linear load

B. Performance of DSTATCOM in Voltage Regulation Mode

The response of shunt compensator for voltage regulation mode under varying load condition is depicted in Fig. 7. In this figure, the waveforms of PCC voltages (v_s), supply currents (i_s), load currents (i_{la}, i_{lb} and i_{lc}), compensator currents (i_{Ca}, i_{Cb} and i_{Cc}), voltage at dc link (V_{dc}) and magnitude of PCC voltage (V_t) are represented. An unbalancing in load is created during t=0.74s to t=0.8s, when phase 'c' of load is disconnected. During unbalancing, it is observed that supply currents are balanced and sinusoidal. The magnitude of PCC voltage is regulated at reference value of 338.8V. After t=0.8s, phase 'c' of load is reconnected and it is observed that PCC voltage achieves its reference value 338.8V within one cycle with the action of PI controller.

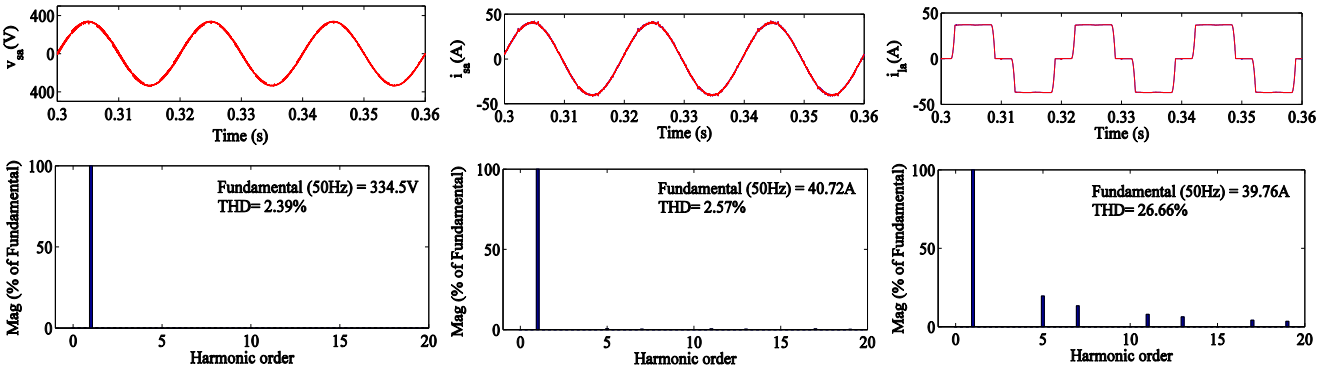

Fig. 6 Waveforms and harmonic spectra of phase 'a' of (a) PCC voltage, v_{sa} (b) supply current, i_{sa} and (c) load current, i_{la} in PFC mode.

This article has been accepted for publication in a future issue of this journal, but has not been fully edited. Content may change prior to final publication. Citation information: DOI 10.1109/TII.2016.2516823, IEEE Transactions on Industrial Informatics

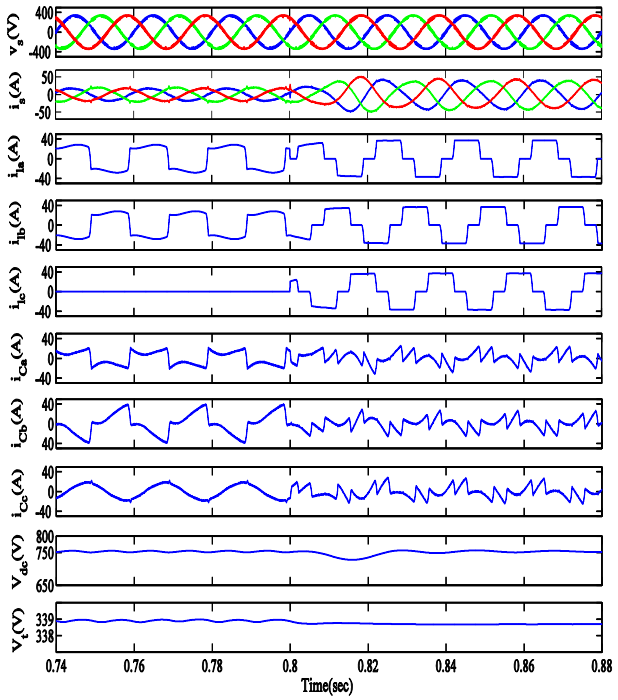

Fig. 7 Performance of compensator for voltage regulation mode under varying nonlinear load

Figs. 8(a)-(c) show harmonic spectra of phase 'a' of PCC voltage (v_{sa}), supply current (i_{sa}) and load current (i_{la}) along with their waveforms respectively. These results depict 2.69%, 2.71 % and 26.83% THD in PCC voltage, supply current and load current respectively. It is observed from these results that supply current achieves 2.71% THD, whereas there is 26.83%THD in load current. These results show the THDs of supply current and PCC voltage within the limit specified by IEEE-519 standard. Fig. 7 and Fig. 8 depict satisfactory performance of DSTATCOM with ANFIS-LMS control algorithm under varying loads in voltage regulation mode.

C. Comparative Performance of ANFIS-LMS Based Control Algorithm

The proposed control algorithm for DSTATCOM is compared with fixed step LMS and variable step LMS (VSLMS). Fig. 9 shows the convergence of fundamental active power weight of load current for ANFIS-LMS, LMS and VSLMS based control algorithms. It is observed from these results in Fig. 9(a) that the extracted weight converges faster and achieves constant value in case of ANFIS-LMS, whereas it oscillates around the mean value in case of LMS and VSLMS control algorithm. Fig. 9(b) shows the performance of all three control algorithms under load unbalancing. It is observed from these results that during load unbalancing (t=0.7s to t=0.8s), an ANFIS-LMS algorithm outputs a converged weight with small oscillation about the mean position. However, the weights obtained with LMS and VSLMS algorithms either do not converge or have large oscillations. Due to sustained and large oscillations in control based on LMS and VSLMS, these algorithms are less stable than ANFIS-LMS especially under unbalanced load conditions. Figs. 10(a) and (b) show the harmonic spectra of supply current (i_{sa}) with LMS and VSLMS based control algorithms respectively. Supply current THDs of 4.29% and 3.62% are obtained with LMS and VSLMS, whereas supply current THD of 2.57% is obtained in ANFIS-LMS based control for PFC mode. It may be concluded from results shown in Figs. 9(a) and (b), Figs. 10(a) and (b) that the performance of ANFIS-LMS based control algorithm is better in terms of convergence and harmonic compensation. The comparative performances of these control algorithms are summarized in Table-I.

V. Experimental Results

An experimental verification of proposed control algorithm is performed on a small scale laboratory prototype of DSTATCOM. The Hall Effect voltage (LV25-P) and current sensors (LA25-NP) are used for sensing of voltages at PCC, voltage at dc link, load currents and supply currents. Two voltage sensors of 10-500V (LEM-LV25-P) are used to sense PCC voltages and one voltage sensor of 10-1500V (LEM-LV25-P/SP5) is required to sense voltage at the dc link. Load and supply currents are sensed using Hall Effect current sensors (LEM LA25-NP). The control algorithm for DSTATCOM is implemented using DSP TMS320F240 (dSPACE1104). The measurements of test results are taken with the power quality analyzer (Fluke 43B) and digital storage oscilloscope (Agilent DSO-X 2014A). Test results are taken for both steady state and dynamic load conditions and design parameters of the system are given in Appendix-B.

A. Performance of ANFIS-LMS Based Control Algorithm for DSTATCOM Under Nonlinear Load

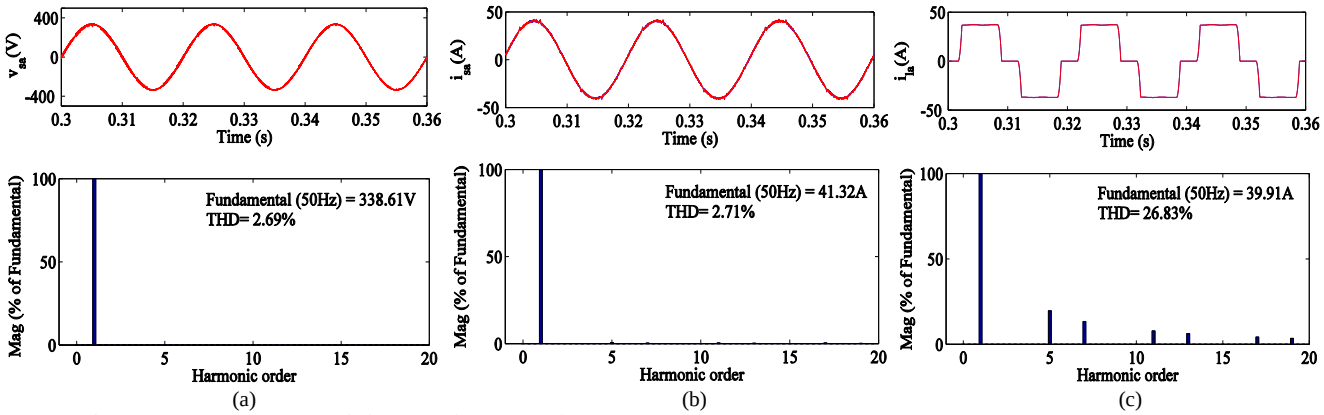

Fig. 8 Waveforms and harmonic spectra of phase 'a' of (a) PCC voltage, v_{sa} (b) supply current, i_{sa} and (c) load current, i_{la} in voltage regulation mode

This article has been accepted for publication in a future issue of this journal, but has not been fully edited. Content may change prior to final publication. Citation information: DOI 10.1109/TII.2016.2516823, IEEE Transactions on Industrial Informatics

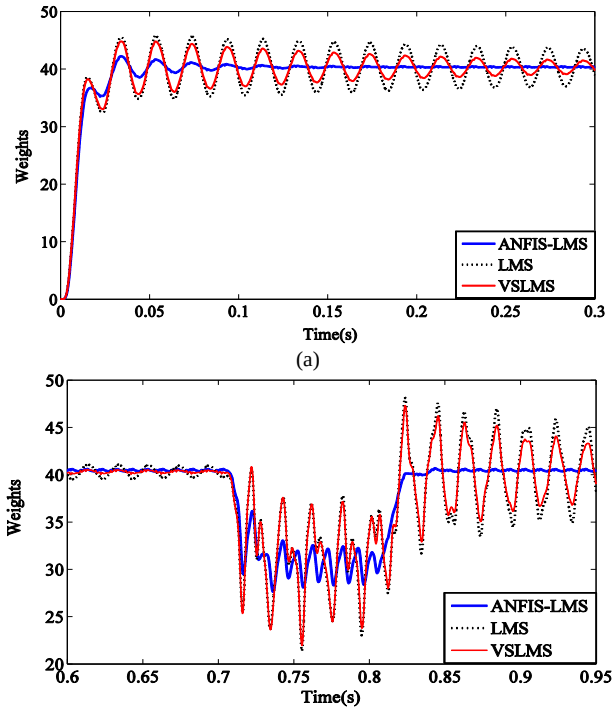

Fig. 9 Comparative performance of weight convergence in (a) steady state (b) unbalanced load condition

Figs. 11(a)-(e) show the performance of proposed ANFIS-LMS based control algorithm for DSTATCOM with intermediate signals. These intermediate signals are presented here to show effectiveness of the control algorithm. Fig. 11(a)

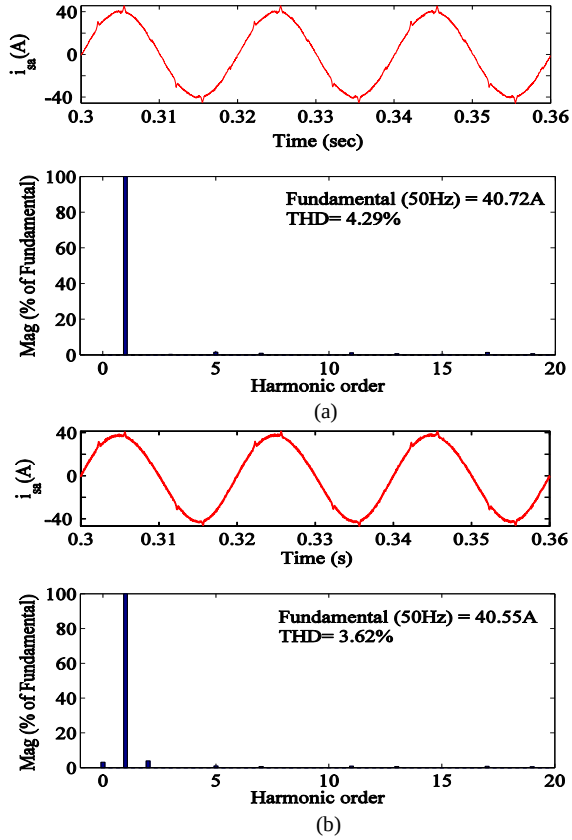

Fig. 10 Harmonic spectra of (a) i_{sa}, For LMS (b) i_{sa}, for VSLMS

TABLE I
COMPARATIVE PERFORMANCE OF ANFIS-LMS BASED CONTROL ALGORITHM

Operation	ANFIS-LMS	LMS	VSLMS
Convergence rate	0.1s	Oscillate around mean value	Oscillate around mean value
Sampling time (T_s)	60µs	50µs	60µs
Step size (µ)	Variable	Fixed	Variable
Static error	Less due to variable µ	Large	In between
THD obtained	Supply current, 40.72A, 2.57%	Supply current, 40.72A, 4.29%	Supply current, 40.55A, 3.62%
	Load current, 39.76A, 26.66%	Load current, 39.76A, 26.66%	Load current, 39.76A, 26.66%

shows the phase 'a' of PCC voltage (v_{sa}) and its filtered value (v_{sa1}) along with phase 'c' of load current (i_{lc}) and average value of active power weight (w_{pavg}). Fig. 11(b) shows error (e), change in error (Δe), variable step size (µ) along with unit in phase component of phase 'a' of PCC voltage (u_{pa}). Fig. 11(c) shows output of dc bus PI controller (w_{ploss}), average active power weight (w_{pavg}), reference active power weight (w_p) along with output of dc bus PI controller (V_{dc}). Fig. 11(d) shows weights corresponding to fundamental active power components of three phase load currents (w_{ap}, w_{bp} and w_{cp}) along with their average weight (w_{pavg}). These results are shown in varying load conditions when phase 'c' of load current is switched off. It is observed from these results that intermediate signals such as fundamental active power weights and their average value are converged to the optimum value in steady state and unbalanced load condition within few cycles. Fig. 11(e) shows reference currents (i_{sa}^*, i_{sb}^* and i_{sc}^*) along with filtered PCC voltage (v_{sa1}). These three-phase reference supply currents are observed to be perfectly sinusoidal and in phase with respective PCC voltages. These results show satisfactory performance of ANFIS-LMS in power factor correction mode for control of shunt compensator.

B. Performance of DSTATCOM Under Steady State Conditions

Fig. 12 depicts the behavior of DSTATCOM under steady state condition. These results show the effectiveness of DSTATCOM in compensating distorted load currents and maintaining supply current sinusoidal with ANFIS-LMS based control algorithm. Figs. 12(a)-(c) show waveforms of the phase 'a' of supply current (i_{sa}), load current (i_{la}) and DSTATCOM current (i_{Ca}) along with PCC voltage (v_{ab}). The harmonic spectra of phase 'a' of supply current (i_{sa}), load current (i_{la}) and PCC voltage (v_{ab}) are shown in Figs. 12 (d)-(f).The THD of 4.9%, 24.7% and 3.9% are obtained in i_{sa}, i_{la} and v_{ab} respectively. It is observed from results shown in Figs. 12(a) and (b) that the supply current (i_{sa}) is sinusoidal and balanced after compensation, whereas the load current (i_{la}) is distorted. Result in Fig. 12(c) shows that harmonic distortion is compensated by shunt compensator. Figs. 12(d) and (f) show THDs of supply current and PCC voltage, which lie within 5% limits as specified by IEEE-519 standard.

This article has been accepted for publication in a future issue of this journal, but has not been fully edited. Content may change prior to final publication. Citation information: DOI 10.1109/TII.2016.2516823, IEEE Transactions on Industrial Informatics

C. Load Balancing Using DSTATCOM

Fig. 13 depicts behavior of compensator under unbalanced load conditions. Figs. 13(a)-(c), (d)-(f) and (g)-(i) show waveforms of supply currents (i_{sa}, i_{sb} and i_{sc}), load currents (i_{la}, i_{lb} and i_{lc}) and compensator currents (i_{Ca}, i_{Cb} and i_{Cc}) along with PCC voltage (v_{ab}). Figs.13(a)-(c) show sinusoidal and balanced supply currents, when phase 'c' of load current is removed to create load unbalancing. Results shown in Figs. 13(g)-(i) present that the unbalanced current is completely provided by the shunt compensator. The proposed ANFIS-LMS based control algorithm for DSTATCOM regulates grid currents sinusoidal even under load unbalancing.

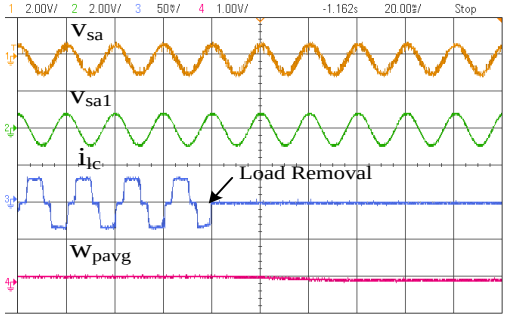

(a)

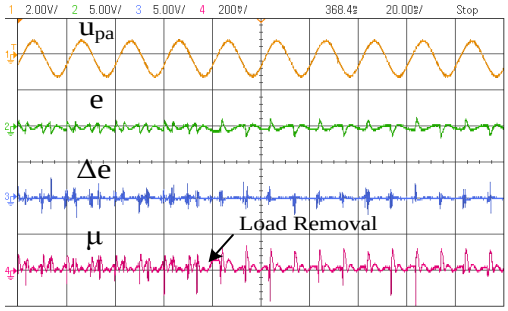

(b)

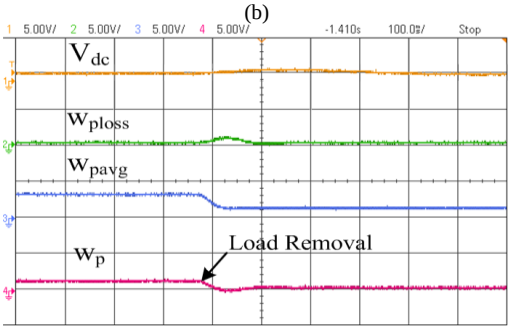

(c)

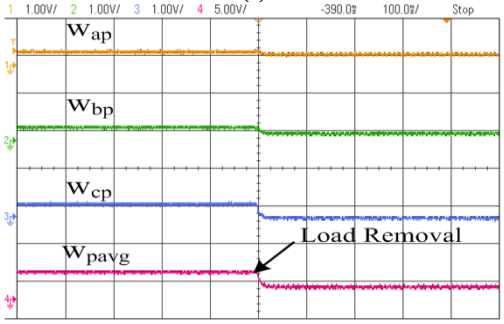

(d)

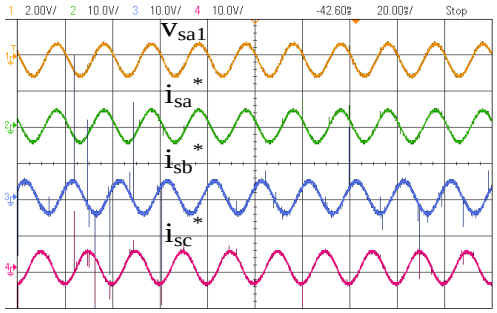

(e)

Fig. 11 Intermediate signals for dynamic load condition under nonlinear load (a) v_{sa}, v_{sa1} i_{lc} and w_{pavg} (b) u_{pa}, e, Δe and μ (c) V_{dc}, w_{ploss}, w_{pavg} and w_p (d) w_{ap}, w_{bp}, w_{cp} and w_{pavg} (e) v_{sa1}, i_{sa}^*, i_{sb}^* and i_{sc}^*

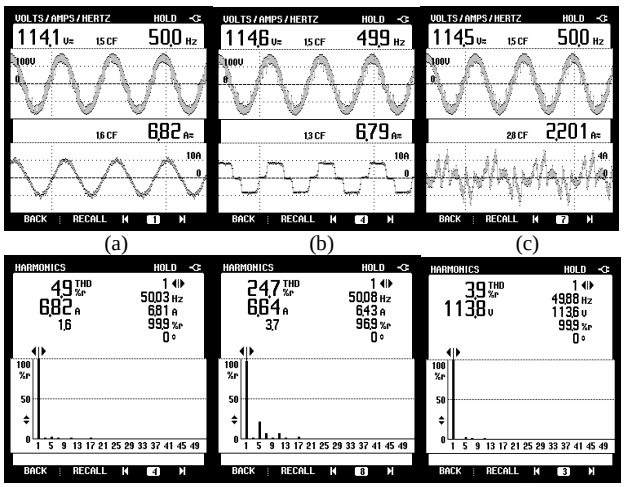

(a) (b) (c) (d) (e) (f)

Fig. 12 Steady state performance of DSTATCOM under nonlinear load (a) v_{ab} and i_{sa} (b) v_{ab} and i_{la} (c) v_{ab} and i_{Ca} (d) harmonic spectrum of i_{sa} (e) harmonic spectrum of i_{la} and (f) harmonic spectrum of v_{ab}.

D. Dynamic Performance of DSTATCOM

The dynamic performance of shunt compensator is recorded

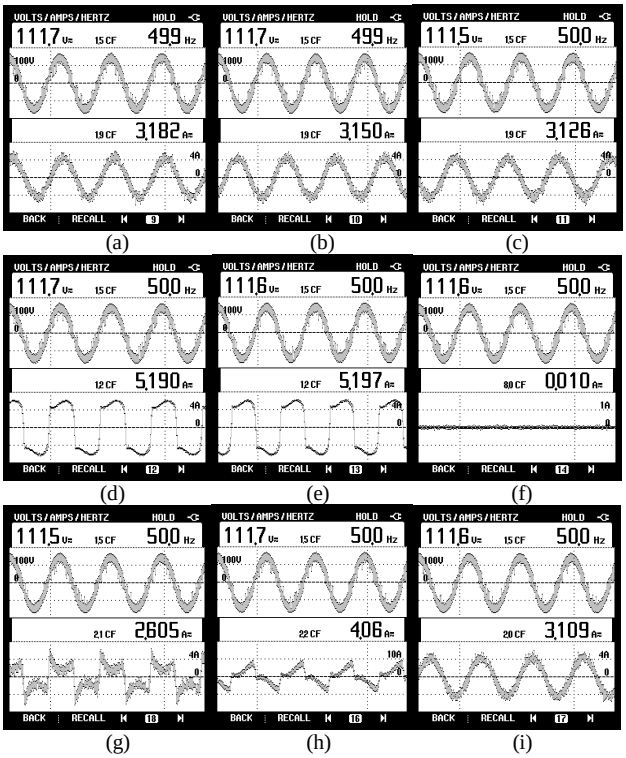

(a) (b) (c) (d) (e) (f) (g) (h) (i)

Fig. 13 Load balancing using DSTATCOM with unbalanced nonlinear load (a-c) i_{sa} , i_{sb} , and i_{sc} with v_{ab} (d-f) i_{la} , i_{lb}, and i_{lc} with v_{ab} (g-i) i_{Ca} ,i_{Cb}, and i_{Cc} with v_{ab}.

This article has been accepted for publication in a future issue of this journal, but has not been fully edited. Content may change prior to final publication. Citation information: DOI 10.1109/TII.2016.2516823, IEEE Transactions on Industrial Informatics

with oscilloscope and depicted in Fig. 14. Figs. 14(a)-(c), show waveforms of supply currents (i_{sa}, i_{sb} and i_{sc}), load currents (i_{la}, i_{lb} and i_{lc}) and DSTATCOM currents (i_{Ca}, i_{Cb} and i_{Cc}) along with filtered PCC voltage (v_{sa1}) under both steady state and unbalanced load conditions. It is observed from these results that the supply currents are sinusoidal and balanced with reduced magnitude, when phase 'c' of load is disconnected. Figs. 14(d) and (e) show waveforms of voltage at dc link (v_{dc}), phase 'c' of supply current (i_{sc}), phase 'c' of load current (i_{lc}) and phase 'c' of compensator current (i_{Cc}) in balanced and unbalanced load conditions for both load removal and load added respectively. It is observed from these results that under dynamic load conditions such as removal of one phase or addition of one phase load, the voltage at dc link achieves its reference value of 200V within few cycles. The testing of DSTATCOM under worst form of unbalancing (one phase load removal) ensures satisfactory performance of DSTATCOM under varying load conditions.

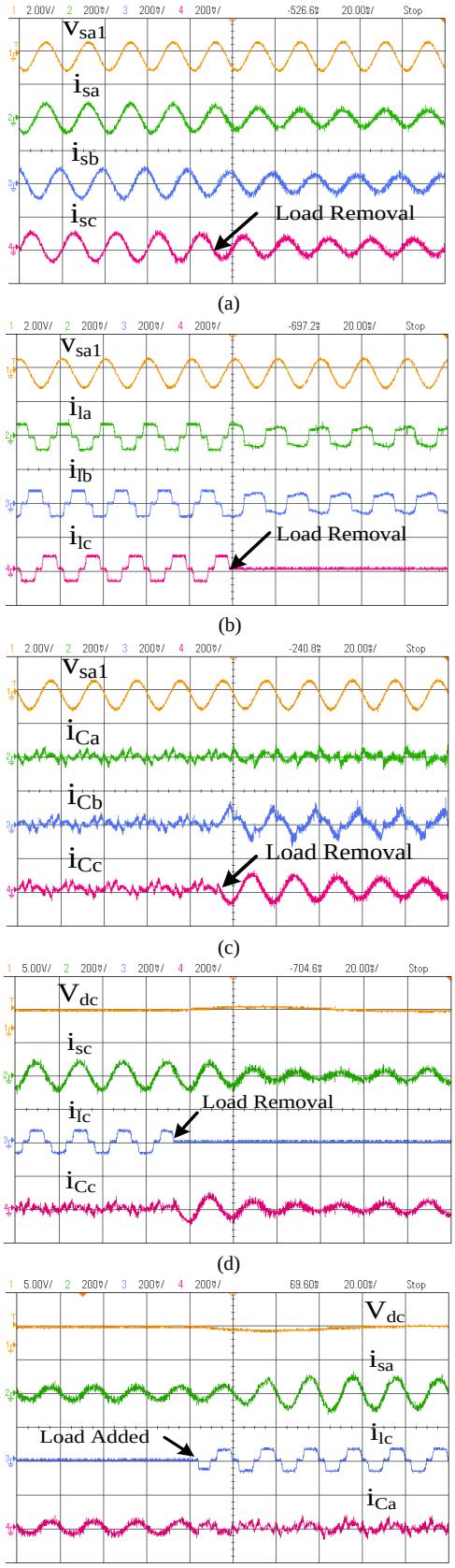

Fig. 14 Performance of shunt compensator for dynamic load condition under nonlinear load (a) v_{sa}, i_{sa}, i_{sb} and i_{sc} (b) v_{sa}, i_{la}, i_{lb} and i_{lc} (c) v_{sa}, i_{Ca}, i_{Cb} and i_{Cc} (d) V_{dc}, i_{sc}, i_{lc} and i_{Cc} for load removal (e) V_{dc}, i_{sc}, i_{lc} and i_{Cc} for load added

VI. Conclusion

The ANFIS-LMS based control algorithm has been verified for the control of three phase shunt compensator. This algorithm has been used to extract reference supply currents from non-sinusoidal load currents. The performance of DSTATCOM using ANFIS-LMS based control has been found to be satisfactory for PFC and voltage regulation modes under varying load conditions. The power quality problems such as harmonics, reactive power and load unbalancing have been mitigated using DSTATCOM. The THD in supply current has been reduced to 2.57% when there is THD of 26.66% in load current. The DSTATCOM has been able to achieve improved power quality and after compensation the THD in supply currents lies within the limit specified by IEEE-519 standard. The magnitudes of voltages at PCC and dc bus have been regulated to their reference values under steady state and unbalancing load conditions. The ANFIS-LMS based control algorithm has been compared with fixed step LMS and VSLMS control algorithms. The proposed algorithm has advantages over other two in terms of fast convergence, less static error and fast learning of step size parameter.

Appendix-A

Rating of AC mains: 415V, three phase and 50 Hz; source impedance R_s=0.05Ω, L_s=1mH; VSC rating 25kVA; value of ripple filters R_f=5Ω, C_f=5μF; value of interfacing inductor L_f=3.4mH; value of dc link capacitor C_{dc}=1650μF; Voltage at dc bus V_{dc}=750V; dc bus PI gains k_{pd}=0.3, k_{id}=0.7; gains of PI for voltage regulation k_{pq}=0.015, k_{iq}=0.001; three phase uncontrolled diode rectifier with R=15Ω and L=100mH; cutoff frequency of LPF used for dc bus voltage=12Hz; cutoff frequency of LPF used for PCC voltage magnitude=10Hz.

Appendix-B

Rating of AC mains 110V, 3-phase and 50 Hz; value of interfacing inductor L_f=3.4mH; value of dc link capacitor C_{dc}=1650μF; voltage at dc bus V_{dc}=200V; 3-phase

This article has been accepted for publication in a future issue of this journal, but has not been fully edited. Content may change prior to final publication. Citation information: DOI 10.1109/TII.2016.2516823, IEEE Transactions on Industrial Informatics

uncontrolled rectifier with R varies from 18 to 60 Ω and L=100mH; sampling time T_s=60μs.

REFERENCES

[1] J. Schlabbach, D. Blume and T. Stephanblome, *Voltage Quality in Electrical Power Systems*. ser. PEE Series. New York: IEE Press, 2001.

[2] A. Ghosh and G. Ledwich, *Power Quality Enhancement using Custom Power Devices.* Springer International Edition, Delhi, 2009.

[3] B. Singh, A. Chandra and K. Al-Haddad, *Power Quality: Problems and Mitigation Techniques*, John Wiley and Sons, U.K., 2015.

[4] B. Singh, P. Jayaprakash, D.P. Kothari, A. Chandra, and K. Al Haddad, "Comprehensive study of DSTATCOM configurations," *IEEE Trans. Ind. Inform.*, vol. 10, no. 2, pp. 854-870 , May 2014.

[5] W. Shireena and T. Li, "A DSP-based active power filter for low voltage distribution systems," *J. Electr. Pow. Syst. Res.*, vol.78, 1561–1567, 2008.

[6] C. Kumar and M.K. Mishra, "A multifunctional DSTATCOM operating under stiff source," *IEEE Trans. Ind. Electron.*, vol. 61, no. 7, pp. 3131-3136, July 2014.

[7] H. Akagi, Y. Kanazawa, and A. Nabae, "Generalized theory of the instantaneous reactive power in three-phase circuits," in *Proc. IEEE and JIEE IPEC*, 1983, pp. 821–827.

[8] M. Popescu, A. Bitoleanu, and V. Suru, "A DSP-based implementation of the p–q theory in active power filtering under nonideal voltage conditions," *IEEE Trans. Ind. Informat.*, vol. 9, no. 2, pp. 880–889, May 2013.

[9] B. Singh and V. Verma, "Selective compensation of power-quality problems through active power filter by current decomposition," *IEEE Trans. Pow. Del.*, vol. 23, no. 2, April 2008.

[10] S. Bhattacharya, D. M. Divan, and B. Banerjee, "Synchronous frame harmonic isolator using active series filter," in *Proc. EPE*, 1991, pp. 3030–3035.

[11] C. H. da Silva, R. R. Pereira, L. E. B. da Silva, G. Lambert-Torres, B. K. Bose, and S. U. Ahn, "A digital PLL scheme for three-phase system using modified synchronous reference frame," *IEEE Trans. Ind. Electron.*, vol. 57, no. 11, pp. 3814–3821, Nov. 2010.

[12] S. Akhtar and D. S. Bernstein, "Lyapunov-stable discrete-time model reference adaptive control," *Int. J. Adaptive Contr. Signal Proc.*, vol. 19, pp. 745–767, 2005.

[13] V. Khadkikar, A. Chandra, and B.N. Singh, "Generalised single-phase p-q theory for active power filtering: simulation and DSP-based experimental investigation," *IET Power Electron.*, vol. 2, no. 1, pp. 67–78, 2009.

[14] B. Singh and S. Arya, "Software PLL based control algorithm for power quality improvement in distribution system," in *Proc. IEEE IICPE-2012*, pp. 1-6.

[15] M. Angulo, D.A. Ruiz-Caballero, J. Lago, M.L. Heldwein, and S.A. Mussa, "Active power filter control strategy with implicit closed-loop current control and resonant controller," *IEEE Trans. Ind. Electron.*, vol. 60, no. 7, pp. 2721-2730 , July 2013.

[16] B. Singh and J. Solanki, "An implementation of an adaptive control algorithm for a three-phase shunt active filter," *IEEE Trans. Ind. Electron.*, vol. 56, no. 8, pp. 2811–2820, Aug. 2009.

[17] B. Singh and S. Arya, "Adaptive theory-based improved linear sinusoidal tracer control algorithm for DSTATCOM," *IEEE Trans. Powe. Electron.*, vol. 28, no.8, pp. 3768-3778, Aug. 2013.

[18] Mu Longhua, Jiangzi, "Application of adaptive filtering in harmonic analysis and detection," in *Proc. of IEEE/PES Transmission and Distribution Conference and Exhibition*, Asia and Pacific Dalian, China, 2005, pp. l-4.

[19] H. Li, Z. Wu, and F. Liu, "A novel variable step-size adaptive harmonic detecting algorithm applied to active power filter," in *Proc. IEEE ICIT, Mumbai, India*, 2006, pp. 574–578.

[20] T. Aboulnasr and K. Mayyas, "A robust variable learning rate LMS-type algorithm: analysis and simulations", *IEEE Trans. Signal Process.*, vol. 45, no. 3, pp. 631–639, 1997.

[21] Y. Qu, W. Tan, Y. Dong, and Y. Yang, "Harmonic detection using fuzzy LMS algorithm for active power filter," in *Proc. IEEE IPEC*, Singapore, 2007, pp. 1065–1069.

[22] B. Farhang-Boroujeny, *Adaptive Filters: Theory and Applications*. Chichester, U.K., Wiley, 1998.

[23] S. Arya and B. Singh, "Neural network based conductance estimation control algorithm for shunt compensator," *IEEE Trans. Ind. Inform.*, vol. 10, no. 1, pp. 569–577, Feb. 2014.

[24] M. Qasim and V. Khadkikar, "Application of artificial neural networks for shunt active power filter control," *IEEE Trans. Ind. Inform.*, vol. 10, no. 3, pp. 1765-1774 , Aug. 2014.

[25] R. L. de Araujo Ribeiro, C. C. de Azevedo, and R. M. de Sousa, "A robust adaptive control strategy of active power filters for power-factor correction, harmonic compensation, and balancing of nonlinear loads," *IEEE Trans. Pow Electron.*, vol. 27, no. 2, Feb. 2012.

[26] M. Singh and A. Chandra, "Real-time implementation of ANFIS control for renewable interfacing inverter in 3P4W distribution network," *IEEE Trans. Ind. Electron.*, vol. 60, no.1, Jan. 2013.

[27] J. S. R. Jang and C. T. Sun, "Neuro-fuzzy modeling and control," *Proc. IEEE*, vol. 83, no. 3, pp. 378–406, Mar. 1995.

[28] J.S.R. Jang, "ANFIS: Adaptive-network-based fuzzy inference system," *IEEE Trans. Syst. Man, Cybern.*, vol. 23, no. 3, pp. 665–685, May/Jun. 1993.

Manoj Badoni received the B. Tech. in Instrumentation Engineering form University Science and Instrumentation Centre (USIC), Srinagar Garhwal, Uttrakhand in 2006 and M.E. degree in Electronics Engineering from Punjab Engineering College (PEC), Chandigarh, India in 2008. He is currently working towards the Ph.D Degree in the Electrical Engineering Department of Delhi Technological University, Delhi, India. His areas of research interest include power electronics, power quality, and distributed generation.

Alka Singh (SM'15) received the B.E. in Electrical Engineering from Delhi College of Engineering, Delhi, India in 1996, M.Tech. in Power Systems from the Indian Institute of Technology, New Delhi, India in 2001 and Ph.D from Netaji Subash Institute of Technology (Delhi University), Delhi, India in 2006. She is currently working as an Associate Professor in the Department of Electrical Engineering, Delhi Technological University, Delhi. Her research interests include FACTS, power systems and power quality. She has over fifteen years of teaching and industrial experience. She is a IEEE Senior member and Life Member of the Indian Society for Technical Education.

Bhim Singh (SM'99–F'10) received the B.E. (Electrical) degree from the University of Roorkee, Roorkee, India, in 1977 and the M.Tech. (Power Apparatus & Systems) and Ph.D. degrees from the Indian Institute of Technology (IIT) Delhi, New Delhi, India, in 1979 and 1983, respectively. In 1983, he joined the Department of Electrical Engineering, University of Roorkee, as a Lecturer. He became a Reader there in 1988. In December 1990, he joined the Department of Electrical Engineering, IIT Delhi, as an Assistant Professor, where he became an Associate Professor in 1994 and a Professor in 1997. He has guided 59 Ph.D. dissertations and 156 M.E./M.Tech theses. He has been granted one U.S. patent and filed 17 Indian patents. He has executed more than 75 sponsored and consultancy projects. Prof. Singh is a Fellow of the Indian National Academy of Engineering, the National Science Academy, the Indian Academy of Science, the Institute of Engineering and Technology, U.K., the Institution of Engineers (India), the World Academy of Sciences (FTWAS), the Indian National Science Academy, and the Institution of Electronics and Telecommunication Engineers. He has also received Shri Om Prakash Bhasin Award-2014 in the field of Engineering including Energy & Aerospace.